NMR Spin Dynamics in Solids. II. Pulse Experiments in Two-Spin-Species Systems*

P. Mansfield, K. H. B. Richards, and D. Ware†

Department of Physics, University of Nottingham, Nottingham, England

(Received 29 August 1969)

A theoretical and experimental study is made of the response of a two-ingredient spin system when repeatedly pulsed at resonance by a number of 90° rf pulses. With a long train of 90° pulses, a sustained chain of solid echoes was produced for Na^{23} in NaF. The peak echo amplitude was found to decay non-exponentially for short times (i.e., the first few echoes), settling down for long times to an exponential decay characterized by a time constant $T_{2\epsilon}$. A theoretical expression for $T_{2\epsilon}$ derived in a similar manner to that for a single-ingredient spin system, described previously by Waugh and Wang and by Mansfield and Ware, does not fit the experimental data. A more general theoretical approach to the multiple-pulse experiments is developed, based on the use of a logarithmic operator. Using this formalism together with a line-narrowing model similar to Anderson's theory of spectral line narrowing in solids in the presence of an exchange interaction, a new expression for $T_{2\epsilon}$ is derived. Some related long-pulse experiments have been performed in which the Na^{23} magnetization following an initial 90° pulse is spin-locked in a low rf field. These experiments simulate the mean rf field in the multiple-pulse experiment. Oscillation of the spin-locked magnetization is observed. Theoretical expressions are derived which describe these oscillations, and their relation to the multiple-pulse experiments is discussed. Mentioned briefly are some multiple-pulse experiments on F^{19} in CaF_2 doped with paramagnetic impurities; also discussed briefly are some earlier multiple-pulse double-resonance experiments carried out on both nuclear species in NaF.

I. INTRODUCTION

THE response of a solid with one nuclear species to a train of in-phase 90° rf pulses has been studied extensively by Waugh and Wang[1] and Mansfield and Ware[2] (hereafter referred to as I). In both of these papers, it was demonstrated that the action of these pulse trains was to produce a sustained chain of solid echoes, thus effectively slowing down the transverse decay. The echo peaks were found to decay exponentially with time constant $T_{2\epsilon}$. The magnitude of $T_{2\epsilon}$ and its dependence on the 90° pulse spacing τ was explained satisfactorily by invoking the symmetry properties of the dipolar Hamiltonian under 90° rotations and assuming the density matrix describing the spin system at the even echo maxima was in an attenuated diagonal state.

In the present paper, which is an extension of our previous work I, we study the response of spin systems with two nuclear species I and S. In the multiple-pulse experiments the rf field is assumed to interact with one species only.

Multiple-pulse experiments performed on Na^{23} in NaF show the solid-echo chain to be nonexponential for short times corresponding to the first few echo peaks. For long times, the echo chain settles down to an exponential behavior. From the echo behavior it is evident that any theory for $T_{2\epsilon}$ based on a reiterative procedure or an attenuated diagonal density matrix at successive solid-echo peaks must fail. The echo be-havior is surprisingly quite different to that of a single species system, and has necessitated further theoretical work.

In Sec. II a theoretical approach to the calculation of the multiple-pulse response is developed based on the use of a logarithmic operator. With this, certain results are proved to all orders in the perturbation expansion. Using this formalism, a line narrowing theory is developed, analogous to Anderson's theory[3] of spectral line narrowing in solids. From this a new expression for $T_{2\epsilon}$ is obtained.

Quite recently, a variety of multiple-pulse experiments have been proposed and performed[4-12] in which the rf phase of successive pulses is modulated in various ways. The prime object of these experiments is to remove or partially reduce the effect of the dipolar interaction in materials where small chemical shifts between two or more chemically inequivalent sites are normally masked by a much larger dipolar interaction. These experiments are of course special cases of multiple-ingredient systems in which the rf pulses interact equally with all spins. The theoretical formalism developed in this paper is also applicable to these experiments, and is discussed briefly. Our main discussion however, is centered on the 90° pulse in-phase sequences.

[1] J. S. Waugh and C. H. Wang, Phys. Rev. **162**, 209 (1967).
[2] P. Mansfield and D. Ware, Phys. Rev. **168**, 318 (1968).
[3] P. W. Anderson, J. Phys. Soc. Japan **9**, 316 (1954).
[4] P. Mansfield and D. Ware, Phys. Letters **22**, 133 (1966).
[5] J. S. Waugh and L. M. Huber, J. Chem. Phys. **47**, 1862 (1967).
[6] P. Mansfield and D. Ware, Phys. Letters **27A**, 159 (1968), and references therein.
[7] J. S. Waugh, C. H. Wang, L. M. Huber, and R. L. Vold, J. Chem. Phys. **48**, 662 (1968).
[8] W. A. B. Evans, Ann. Phys. (N.Y.) **48**, 72 (1968).
[9] J. S. Waugh, L. M. Huber, and U. Haeberlen, Phys. Rev. Letters **20**, 180 (1968).
[10] U. Haeberlen and J. S. Waugh, Phys. Rev. **175**, 453 (1968).
[11] D. Ellett, U. Haeberlen, and J. S. Waugh, Polymer Letters **7**, 71 (1969).
[12] P. Mansfield and K. H. B. Richards, Chem. Phys. Letters **3**, 169 (1969).

We also present a theoretical and experimental study of some related experiments in which the magnetization following an initial intense 90° rf pulse is rapidly spin-locked in a long low-power rf pulse at resonance. The magnetization is found to oscillate as a function of the spin-locking time, damping out to a quasiequilibrium value, which is close to the thermal-equilibrium value. These experiments are intended to simulate the multiple-pulse experiments by replacing the 90° pulse train by its mean field. They explain physically the slight ripple observed in the solid-echo chains in terms of mutual exchange of magnetic energy between the dipolar and Zeeman reservoirs.

An extension of the long-pulse theory given in I to the case of two spin species shows that in addition to the oscillatory term obtained in the single-ingredient case, a term with roughly twice the period appears. Phenomenologically, the oscillations in a single-ingredient system may be ascribed to classical precession of the spins about a distribution of effective fields made time-dependent through the spin-flip terms in the dipolar Hamiltonian. For a well-resolved two-species system, however, the spin-flip term between spin species is quenched. Thus part of the precessional motion of the resonant spins will be about a distribution of static effective fields at the usual Larmor angular frequency.

A brief discussion of some multiple-pulse double-resonance results[13] is given in which both the Na^{23} and F^{19} nuclei in a single crystal of NaF are simultaneously irradiated. These experiments are analogous to the double-resonance experiments of Hartmann and Hahn[14] and of Lurie and Slichter.[15] Also discussed are some preliminary results of multiple-pulse experiments on paramagnetically doped samples.

II. THEORY

A. Multiple-Pulse Analysis

We wish to calculate the transverse response of a spin system consisting of two magnetic ingredients with spin numbers I and S, initially in thermal equilibrium in a large static magnetic field $\mathbf{H}_0$, when irradiated at the resonance frequency of the I spins by a number of 90° rf pulses. The basic formalism is similar to our previous Paper I.

We denote the rf pulse sequence as 90°-τ-90°$_{90°}$-(2τ-90°$_{90°}$)$_{N-1}$, where N is the number of phase coherent pulses, τ is the time interval, and the subscript 90° means that the pulse is in rf phase quadrature with the first 90° preparation pulse.

The essential features of the response are calculated in the frame of reference rotating at the Larmor angular frequency ω_0. In this frame the important spin Hamil-

tonian for the present calculation is the dipolar term

$$\hbar\mathcal{3C}_1{}^0 = (\mathcal{E} + \mathcal{F} + \mathcal{G})\hbar, \tag{1}$$

where

$$\mathcal{E} = \sum_{k>j} A_{jk}\mathbf{I}_j \cdot \mathbf{I}_k + B_{jk}I_{zj}I_{zk},$$

$$\mathcal{F} = \sum_{k,\beta} C_{k\beta}I_{zk}S_{z\beta},$$

$$\mathcal{G} = \sum_{\beta>\alpha} a_{\alpha\beta}\mathbf{S}_\alpha \cdot \mathbf{S}_\beta + b_{\alpha\beta}S_{z\alpha}S_{z\beta}.$$

The coefficients of the spin operators are given by

$$A_{jk} = -\tfrac{1}{3}B_{jk} = -\tfrac{1}{2}\gamma_I{}^2\hbar P_{jk},$$

$$a_{\alpha\beta} = -\tfrac{1}{3}b_{\alpha\beta} = -\tfrac{1}{2}\gamma_S{}^2\hbar P_{\alpha\beta},$$

$$C_{k\beta} = \gamma_I\gamma_S\hbar P_{k\beta},$$

where

$$P_{jk} = 2P_2(\cos\theta_{jk})/r_{jk}{}^3, \text{ etc.}$$

We ignore such matters as spin-lattice relaxation in this analysis. Exchange terms also ignored here would simply add on to the coefficients A_{jk}, $C_{k\beta}$, and $a_{\alpha\beta}$.

If the rf pulse field is made much greater than the effective internal dipolar field, the initial 90° pulse may be represented by a rotation operator $R_0 = e^{i\pi I_y/2}$, i.e., a rotation about the y axis in the rotating frame, the subsequent pulses are all represented by $R_N = e^{i\pi I_x/2}$, i.e., rotations about the x axis.

The two species dipolar Hamiltonian has 360° rotational symmetry, that is to say, a minimum of four 90° rototations recovers the original Hamiltonian, i.e.,

$$R^\dagger\mathcal{3C}_1{}^0 R^4 = \mathcal{3C}_1{}^0.$$

In general, we may write the effect of m rotation operations as

$$(\prod_0^m R_m)^\dagger\mathcal{3C}_1{}^0\prod_0^m R_m = \mathcal{3C}_1{}^m. \tag{2}$$

It is convenient, following Waugh et al.,[7] when considering the long time behavior of the response function, to call the minimum number of pulses m necessary to take $\mathcal{3C}_1{}^0$ through full symmetry a cycle. The cycle period is $\sum_0^m a_m\tau$, where in the present case m runs from 0 to 4 and $a_0 = a_4 = 1$; $a_1 = a_2 = a_3 = 2$.

The transverse response of the spin system to n cycles of m pulses may be conveniently written in terms of a logarithmic operator as

$$\langle I_x \rangle_{nm} = \mathrm{Tr}\{e^{n\ln Q\dagger}I_x e^{n\ln Q}I_x\}, \tag{3a}$$

where $Q^\dagger$ is defined by the ordered product[16]

$$Q^\dagger = \prod_0^m \exp(-i\mathcal{3C}_1{}^m a_m\tau) \equiv \mathcal{O}\exp\sum_0^m -i\mathcal{3C}_1{}^m a_m\tau. \tag{3b}$$

The ordering operator $\mathcal{O}$ means that we must always arrange the Hamiltonian operators $\mathcal{3C}_1{}^m$ in descending

[13] P. Mansfield and D. Ware, Phys. Letters **23**, 421 (1966).
[14] S. R. Hartmann and E. L. Hahn, Phys. Rev. **128**, 2042 (1962).
[15] F. M. Lurie and C. P. Slichter, Phys. Rev. **133**, A1108 (1964).
[16] R. Kubo, J. Phys. Soc. Japan **17**, 1100 (1962).

rank from left to right. The logarithmic operator is formally equivalent to the Magnus expansion as applied to multiple-pulse NMR problems by Evans,[8] but taken to all orders in τ. Introducing the Liouville operator L_n defined by the equation

$$L_n A = [\mathcal{H}_1{}^n, A], \qquad (4)$$

we may write Eq. (3) using the convenient double-square-bracket notation of Waugh and Wang[1] as

$$\langle I_x \rangle_{nm} = \mathrm{Tr}\{(P^n I_x) I_x\} = \mathrm{Tr}\{(e^{n\ln P} I_x) I_x\} \equiv [\![e^{n\ln P}]\!], \qquad (5)$$

where P is defined by the ordered product

$$P = \prod_0^m \exp(iL_m a_m \tau) \equiv \mathcal{O} \exp \sum_0^m iL_m a_m \tau. \qquad (6)$$

As above the ordering operator $\mathcal{O}$ means that we must always arrange the Liouville operators L_m in descending rank from left to right.

It is clear from Eq. (5) that $\ln P$ plays the rôle of a generalized Liouville operator $\mathcal{L}$. From Eqs. (3) and (5) we put

$$(\sum_0^m a_m \tau)\mathcal{L} = \ln P = \ln Q^\dagger + \ln \tilde{Q}, \qquad (7)$$

where the tilde denotes a transposition operation defined by $\tilde{Q}A = AQ$.

In performing calculations it is convenient to expand the operator P in Eq. (6) as follows: We set

$$P = 1 + F(\tau), \qquad (8a)$$

where

$$F(\tau) = \sum_1^l (i\tau)^l \frac{U_l{}^m}{l!} \qquad (8b)$$

and

$$U_l{}^m = \mathcal{O}(\sum_0^m a_m L_m)^l. \qquad (8c)$$

From Eq. (8a) we may formally write the logarithmic operator as

$$\ln P = \sum_1^n (-1)^{p+1} \frac{[F(\tau)]^p}{p}, \qquad (8d)$$

where p and l above are integers.

This particular formalism permits a simple derivation of the mean Hamiltonian limit as used in the papers on the resolution of the chemical shift in solid compounds,[7–12] i.e.,

$$\lim_{\tau \to 0, n \to \infty} (t \ln P / \sum_0^m a_m \tau) = (it U_1{}^m / \sum_0^m a_m),$$

where the real time

$$t = n \sum_0^m a_m \tau$$

is kept finite. Since Eq. (8d) is exact it also forms the

basis for calculations when τ is finite for more complicated pulse cycles[4–12] as well as those discussed here.[17] We emphasize, however, that we have assumed that the rf pulses are effectively δ functions. For finite pulse widths, an analysis along the lines of I Sec. II B or the generalization of Haeberlen and Waugh[10] would be required.

1. First Echo at $t = 2\tau$

This result has been derived previously[18] to higher order, but we rederive it for convenience in our present notation to the lowest nonvanishing order. From Eqs. (5) and (8a)–(8c) we have for the normalized echo amplitude

$$\langle I_x(2\tau) \rangle = [\![1 - U_2{}^1 \tau^2 + \cdots]\!]. \qquad (9a)$$

Generalizing our previous notation for the deviation from unity of the solid-echo amplitude, we write the coefficient of τ^l for the rth echo as $M_{l\epsilon}{}^r$. In this notation Eq. (9a) becomes

$$\langle I_x(2\tau) \rangle = (1 - M_{2\epsilon}{}^1 \tau^2 + \cdots), \qquad (9b)$$

where

$$M_{2\epsilon}{}^1 = M_{2IS} = \frac{\frac{1}{3}S(S+1)}{N_I} \sum_{k,\beta} C_{k\beta}{}^2$$

is the nonresonant spin contribution to the normal Van Vleck second moment. In deriving Eq. (9) we note that for a single-magnetic-ingredient spin system $U_1{}^1 I_x = U_2{}^1 I_x = 0$, whereas for two ingredients $U_2{}^1 I_x \neq 0$.

2. Second Echo at $t = 4\tau$

As in the above case, the leading term is quadratic in τ, and when evaluated gives

$$\langle I_x(4\tau) \rangle = (1 + M_{2\epsilon}{}^2 \tau^2 + \cdots), \qquad (10)$$

where $M_{2\epsilon}{}^2 = -2M_{2IS}$.

3. Third Echo at $t = 6\tau$

From Eqs. (5) and (8) we obtain to fourth order in τ

$$\langle I_x(6\tau) \rangle = (1 + M_{2\epsilon}{}^3 \tau^2 + M_{4\epsilon}{}^3 \tau^4 + \cdots), \qquad (11)$$

where $M_{2\epsilon}{}^3 = -M_{2IS}$. The leading term is thus identical with the first-echo case Eq. (9b). From Eq. (8b) we

---

[17] For example, if we work in the Hamiltonian representation of Eqs. (3a) and (3b), analogous equations to (8a)–(8c) can be generated for $Q^\dagger$, in which L_m is replaced by $\mathcal{H}_1{}^m$ and $U_l{}^m$ is replaced by $V_l{}^m$. Expansion of $\ln Q^\dagger / i\tau \sum_0^m a_m$ then gives

$$\ln Q^\dagger / i\tau \sum_0^m a_m = G(\tau) - [G(\tau)]^2 / 2 + \cdots,$$

where

$$G(\tau) = [V_1{}^m + i\tau V_2{}^m / 2! + \cdots] / \sum_0^m a_m.$$

In the four-pulse cycle proposed by Waugh et al., Ref. 9, which in their notation is $(\tau, P_x, 2\tau, P_{-x}, \tau, P_y, 2\tau, P_{-y})$, where P_α represents a 90° rf pulse applied along the α axis in the rotating frame, it is a simple matter to verify that for the dipolar interaction $V_1{}^4 = V_2{}^4 = 0$. Thus the first two terms in the expansion of $\ln Q^\dagger / i\tau \sum_0^m a_m$ as a power series in τ vanish. This corresponds to the vanishing of the first two Magnus coefficients.

[18] P. Mansfield, Phys. Rev. 137, A961 (1965).

evaluate the fourth-order coefficient $M_{4\epsilon}{}^3 = [\![U_4{}^3]\!]/4!$ by putting $a_0 = a_3 = 1$ and $a_1 = a_2 = 2$. From Eqs. (1), (2), and (4), we introduce sub-Liouville operators defined by

$$L_0 I_x = E I_x + F I_x ,$$
$$L_1 I_x = E' I_x + F' I_x ,$$
$$L_2 I_x = E I_x - F I_x , \qquad (12)$$
$$L_3 I_x = E' I_x - F' I_x ,$$

where E, F, and G introduced later, are the Liouville operators corresponding to $\mathscr{E}$, $\mathscr{F}$, $\mathscr{G}$, and $(E' + F') I_x = R^\dagger (E + F) I_x R$. After a considerable amount of algebra we obtain the result

$$M_{4\epsilon}{}^3 = -\tfrac{1}{12} \{ 33[\![FE^2F]\!] + 44[\![EFEF]\!] + 11[\![EF^2E]\!]$$
$$- 15[\![F^4]\!] - 61[\![F'^2F^2]\!] + 115[\![FG^2F]\!]$$
$$+ 52[\![FE'^2F]\!] + 124[\![FE'EF]\!] - 28[\![EF'EF']\!] \} . \quad (13)$$

4. Fourth Echo at $t = 8\tau$

On expanding Eq. (5) for $n = 1$, using Eqs. (8a)–(8c) only, we find that the leading nonzero term in the fourth-echo expansion has a fourth-power dependence on τ, i.e.,

$$\langle I_x(8\tau) \rangle = (1 + M_{4\epsilon}{}^4 \tau^4 + \cdots) , \qquad (14)$$

where $M_{4\epsilon}{}^4 = [\![U_4{}^4]\!]/4!$. Using Eq. (8c) with $a_0 = a_4 = 1$ and $a_1 = a_2 = a_3 = 2$, noting that $L_0 = L_4$ and making use of the sub-Liouville operators defined in Eq. (12), we find after some straightforward though tedious algebraic manipulation that

$$M_{4\epsilon}{}^4 = -\tfrac{1}{3} \{ 24[\![FE^2F]\!] + 96[\![FG^2F]\!]$$
$$+ 24[\![FE'^2F]\!] + 48[\![FE'EF]\!] \} . \quad (15)$$

The detailed trace evaluation and the lattice sums required to evaluate Eqs. (9a), (10), (11), and (14) numerically have been performed and full details are given in the Appendix.

5. Naive Evaluation of $T_{2\epsilon}$

As in the case of the single magnetic ingredient, we may evaluate the decay time constant of the echo train $T_{2\epsilon}$ by assuming that the semi-spin-locked density matrix is in its most diagonal state when the dipolar Hamiltonian has achieved full symmetry in one cycle, i.e., after four pulses. Of course, the resonant-spin part of the Hamiltonian achieves full symmetry after two pulses, as in I, but our long pulse spin-locking experiments discussed later in Sec. II B suggest that in our particular case, the nonresonant spin contribution to the lattice sums dominates matters. The four-pulse cycle period, therefore, corresponds mainly to precession of spins at the Larmor frequency in the mean pulse field given by $\omega = \gamma_I \bar{H}_p$. There are, of course, components with angular frequency 2ω.

Following the arguments in I, we may evaluate the logarithmic decrement between the nth and $(n+1)$th cycle assuming an exponential decay of the fourth echo

in successive cycles. This approach gives the result

$$T_{2\epsilon} = 8 / M_{4\epsilon}{}^4 \tau^3 . \qquad (16)$$

6. Projection to n Cycles

We may expand P^n in Eq. (5) directly by a Taylor series using Eqs. (8a) and (8b). In this case we obtain for the leading term in τ for the $4n$th echo

$$\langle I_x \rangle_{4n} = [\![1 + [n U_4{}^4 / 4! + \tfrac{1}{8} n(n-1)(U_2{}^4)^2] \tau^4 + \cdots]\!] . \quad (17)$$

It is an easy matter to show that $[\![(U_2{}^4)^2]\!] = 0$, which suggests that the leading term in Eq. (17) is linear in n. This curious result for two spin species is quite different in principle to the result obtained by Waugh and Wang for a single-ingredient spin system. In their case, the leading terms are, of course, sixth order in τ. The analogous expression to Eq. (17) for the $2n$th echo is

$$\langle I_x \rangle_{2n} = [\![1 + [n U_6{}^2 / 6! + n(n-1)(U_3{}^2)^2 / 72]$$
$$\times \tau^6 + \cdots]\!] , \quad (18a)$$

in which

$$[\![U_6{}^2]\!]/6! = [\![(U_3{}^2)^2]\!]/2 \times 3!3! , \qquad (18b)$$

thus leaving in Eq. (18a) the quadratic term in n only.

An alternative procedure for n cycles is to expand Eq. (3) directly in powers of n or expand the logarithmic form of Eq. (5) using Eq. (7). For the $4n$th echo we get

$$\langle I_x \rangle_{4n} = [\![1 + n(\ln Q^\dagger + \ln Q) + n^2(\cdots)]\!] . \qquad (19)$$

Since Q is a unitary operator and $[Q^\dagger, Q] = 0$, we may express the coefficient of n in Eq. (19) as

$$\ln Q^\dagger + \ln Q = \ln Q^\dagger Q = 0 . \qquad (20)$$

This result is quite general for one or two magnetic ingredients and is equally true for an arbitrary operator A instead of I_x, provided Q is unitary. We note that the vanishing of the first moment in the free-induction decay is a special case of the above theorem.

It would seem that the vanishing of the linear term in n shown by Waugh and Wang[1] to be true to sixth order in τ is, in fact, true to infinite order in the time-perturbation expansion. Their result is in a sense fortuitous because of Eq. (18b).

In our case, we have apparently conflicting results. Equation (17) indicates that we have a term linear in n, whereas Eq. (19) and Eq. (20) indicate that we do not. Equation (19), however, is true to infinite order in τ, Eq. (17) is true to fourth order only. This situation exemplifies the dangers of taking the leading term in operator expansions. Thus for two spin species, Eq. (14) although seemingly correct, cannot be true because of Eq. (20).

7. Moment-Cumulant Expansion

In principle, it is a straightforward matter to expand Eq. (5) in powers of real time t, i.e.,

$$\langle I_x(t) \rangle = \sum_r \mathfrak{M}_r(\tau) t^r / r! , \qquad (21)$$

where

$$\mathfrak{M}_r(\tau) = [\![(\ln P/\sum_0^m a_m\tau)^r]\!] = [\![\mathfrak{L}^r]\!].$$

The moments here are functions of τ which all vanish for $r > 0$ and $\tau = 0$. It is well known, however, that straightforward moment expansions are generally slowly converging and, of course, the higher-order moments become extremely tedious to calculate. Provided there are no zeros in the echo amplitude decay, we may, in general, represent Eq. (5) by a cumulant expansion,[2,16] i.e.,

$$[\![e^{\mathfrak{L}t}]\!] \equiv \exp \sum_p K(\mathfrak{L}^p)t^p/p!, \qquad (22)$$

where $K(\mathfrak{L}^p)$ is the pth-order cumulant.

If α is an arbitrary c parameter, and if we denote the differential operator $D_\alpha = \partial/\partial\alpha$, then the cumulants are given by

$$K(\mathfrak{L}^p) = \lim_{\alpha \to 0} D_\alpha{}^p \ln[\![e^{\mathfrak{L}\alpha}]\!][\![1]\!]. \qquad (23)$$

The first few cumulants are therefore

$$K(\mathfrak{L}) = [\![\mathfrak{L}]\!],$$
$$K(\mathfrak{L}^2) = [\![\mathfrak{L}^2]\!] - [\![\mathfrak{L}]\!]^2, \quad \text{etc.} \qquad (24)$$

Now from Eq. (20) it is evident that $K(\mathfrak{L}) = 0$, thus the lowest-order approximation to Eq. (5) is the Gaussian decay

$$\langle I_x(t) \rangle = e^{(1/2)\mathfrak{M}_2 t^2}. \qquad (25)$$

For short times, near the time origin, Eq. (25) is an accurate description of the echo peak envelope. It is precisely here where the diagonal assumption procedure or the iteration procedure must fail, since these assumptions give leading terms linear in t.

For long times, experiment indicates that the echo amplitude decays are closely exponential. The situation here is in many respects similar to the problem of spectral line narrowing in solids by an exchange interaction.[3] The present problem is of course more difficult and complicated by the fact that the odd moments in Eq. (21) do not in general vanish.

8. Effective Line Narrowing by the Mean Hamiltonian

We pursue the exchange narrowing similarity in our problem by writing $\ln P$ in Eq. (5) in two parts; an unordered part $\mathfrak{L}'$ which commutes with I_x, and an ordered part $\mathfrak{L}''$ which does not commute, i.e.,

$$\ln P = (\sum_0^m a_m\tau)[\mathfrak{L}' + \mathfrak{L}''], \qquad (26)$$

where

$$\mathfrak{L}' = \ln(1 + i\tau U_1{}^m)/\sum_0^m a_m\tau,$$

and

$$\mathfrak{L}'' = \sum_1^p \frac{(-1)^{p+1}}{p} \sum_{l_p}'(i\tau)^{\sum l_p} \prod_p \frac{U_{l_p}{}^m}{l_p!} \Big/ \sum_0^m a_m\tau,$$

where p and l_p are integers. (The sum over l_p is restricted, some of the $l_p = 1$ terms having been removed.) Since $\mathfrak{L}'I_x = 0$, the operator $\mathfrak{L}'$, which is in effect the logarithm of the mean field Liouville operator, plays a rôle similar to the exchange interaction in the theory of exchange narrowing in solids. We note that for zero τ the operator $\mathfrak{L}'$ is equal to the Liouville operator of the mean Hamiltonian over the cycle.

As a consequence of Eq. (26) we may write Eq. (5) as a time-ordered product (using the time-ordering operator T)

$$\langle I_x(t) \rangle = \left[\!\!\left[T \exp \int_0^t \mathfrak{L}''(t')dt' \right]\!\!\right], \qquad (27)$$

where $\mathfrak{L}''(t) = e^{-\mathfrak{L}'t}\mathfrak{L}''e^{\mathfrak{L}'t}$. That is to say $\mathfrak{L}''$ is modulated by $\mathfrak{L}'$. Generalizing the cumulant expansion Eq. (22), we introduce a c parameter λ, later to be equated to unity. Combining Eq. (27) and the cumulant expansion definition Eq. (22) we obtain

$$\left[\!\!\left[T \exp\lambda \int_0^t \mathfrak{L}''(t')dt' \right]\!\!\right] \equiv \exp \sum_p K(\mathfrak{L}''(t)^p)\lambda^p/p!, \qquad (28)$$

where the time-dependent cumulants are defined by a similar equation to Eq. (23). The first few cumulants are

$$K[\mathfrak{L}''(t)] = \int_0^t [\![\mathfrak{L}''(t')]\!]dt', \qquad (29a)$$

$$K[\mathfrak{L}''(t)^2] = \int_0^t \int_0^{t'} [\![\mathfrak{L}''(t')\mathfrak{L}''(t'')]\!]dt' \, dt''$$
$$- \left(\int_0^t [\![\mathfrak{L}''(t')]\!]dt'\right)^2. \qquad (29b)$$

Because of the property $\mathfrak{L}'I_x = 0$, it is evident that

$$K[\mathfrak{L}''(t)] = 0 \qquad (30a)$$

and that

$$K[\mathfrak{L}''(t)^2] = K[\mathfrak{L}(t)^2]$$
$$= \int_0^t \int_0^{t'} [\![\mathfrak{L}(t')\mathfrak{L}(t'')]\!]dt' \, dt''. \qquad (30b)$$

The lowest-order cumulant approximation to Eq. (28) is thus similar to Eq. (25). The difference is that now we have time correlation between the two generalized Liouville operators which is brought about by the time dependence of $\mathfrak{L}''$ through $\mathfrak{L}'$. If we assume that the higher-order cumulants are negligible since they represent higher-order correlations which probably average to zero faster, then we have a close analogy to the Anderson theory of exchange narrowing.[3] The analogy

is exact if $\mathcal{L}''$ represents the pure dipole interaction and $\mathcal{L}'$ the exchange term. In Anderson's case, he assumed the dipolar line shape without exchange was Gaussian. We make a similar Gaussian assumption though in our case it is far from certain that if $\mathcal{L}'$ were not present the whole of the echo-train decay would be Gaussian. It is clear from Eq. (25) that initially it is Gaussian.

9. Stochastic Assumption

From the form of the time dependence of $\mathcal{L}(t)$ in the double integral Eq. (30b) we may write the double-time correlation in terms of the difference of the two times. We then assume that we may write

$$[\mathcal{L}(t')\mathcal{L}(t'')] = [\mathcal{L}^2]g(t'-t'') . \tag{31}$$

Substituting $T = t' - t''$ and from a consideration of the domain of integration we may write Eq. (30b) as

$$K[\mathcal{L}(t)^2] = [\mathcal{L}^2] \int_0^t (t-T)g(T)dT . \tag{32}$$

Extension to higher-order cumulants and hence higher-order correlation functions is in principle straightforward. In the present work we restrict our discussion to double-time correlations only. The choice of the correlation function $g(T)$ is to some extent arbitrary. In Anderson's theory of exchange narrowing in solids, $g(T)$ was chosen to be a Gaussian function. This choice satisfies the condition in normal line-shape theory that the odd Van Vleck moments vanish. In our case, as discussed in Sec. II A 7, apart from the first moment, the odd moments $\mathfrak{M}_r$ do not in general vanish. A convenient analytical form of $g(T)$ which embraces this circumstance is the exponential correlation function

$$g(T) = e^{-|T|/\tau_c}, \tag{33}$$

where τ_c is the characteristic correlation time.

Substitution of Eq. (33) into Eq. (32) and of Eq. (32) into Eq. (28) gives for the echo-train decay

$$\langle I_x(t) \rangle = \exp\{\mathfrak{M}_2[\tau_c^2(e^{-t/\tau_c}-1)+t\tau_c]\} . \tag{34}$$

For $t \gg \tau_c$, i.e., for long times, this gives

$$\langle I_x(t) \rangle = e^{\mathfrak{M}_2\tau_c t} = e^{-t/T_{2\epsilon}} . \tag{35a}$$

For $t \ll \tau_c$, i.e., for short times, we get

$$\langle I_x(t) \rangle = e^{(1/2)\mathfrak{M}_2 t^2}, \tag{35b}$$

in agreement with Eq. (25).

Expanding Eq. (34) in powers of t and equating with the moment expansion Eq. (21), we get for the coefficient of t^3

$$\mathfrak{M}_3(\tau) = -\mathfrak{M}_2(\tau)/\tau_c . \tag{36}$$

From Eq. (36) and Eq. (35a) we obtain a new expression for the decay time constant of the solid-echo chain,

$$T_{2\epsilon} = \mathfrak{M}_3(\tau)/[\mathfrak{M}_2(\tau)]^2 . \tag{37}$$

To get some idea of the τ dependence of $T_{2\epsilon}$, we must expand the quotient in Eq. (37) using Eq. (21) and Eqs. (8a)–(8c). Since $[(U_2^4)^2] = 0$, the lowest-order non-zero averages for a two-species system give

$$\mathfrak{M}_3 = [-(U_2^4)^3\tau^3/8 + U_3^4 U_2^4 U_3^4 \tau^5/72 + \cdots]/8^3 \tag{38a}$$

and

$$\mathfrak{M}_2 = [-(U_3^4)^2\tau^4/36 + (U_4^4)^2\tau^6/4!4! + \cdots]/8^2 . \tag{38b}$$

We assume these averages are all nonzero since they do not disappear by symmetry arguments or obvious commutations. Substituting these moments into Eq. (37) we obtain

$$T_{2\epsilon} = \frac{144[U_3^4 U_2^4 U_3^4]}{[(U_3^4)^2]^2\tau^3} - \frac{36^2[(U_2^4)^3]}{[(U_3^4)^2]^2\tau^5} + \cdots . \tag{39}$$

Explicit evaluation of Eq. (39) has not been undertaken since it involves detailed calculation of sixth-moment-like and eighth-moment-like averages for a two-magnetic-ingredient spin system.

B. Long-Pulse Spin-Locking Experiments

As discussed in detail previously in I, the in-phase multiple-pulse sequence rf field envelope may be Fourier analyzed into a zero-frequency component plus side-bands at the harmonic frequencies given by the inverse pulse spacing 2τ. In this section we consider the effect of spin-locking the magnetization by the zero-frequency component only, i.e., we treat the case when the spin system is initially irradiated with an intense 90° rf pulse followed by a long low-power pulse in rf phase quadrature. The detailed formalism is of course similar to that in I. The differences arise since we treat here the case of a spin system with two magnetic ingredients, the resonant species having spin I, the nonresonant having spin S.

In the following calculation, spin-lattice relaxation effects are neglected. This is valid if the total time of the experiment is less than the spin-lattice relaxation time in the rotating frame $T_{1\rho}$.

We wish to calculate the evolution of the spin-locked magnetization following the initial pulse. We perform the calculation in the tilted rotating reference frame, in which the Von Neumann equation of motion of the density matrix ρ is

$$\frac{d\rho}{dt} = -i[\omega_{\text{reff}}I_z + \sum_M G_M, \rho], \tag{40}$$

where $\omega_{\text{reff}} = \sqrt{(\Delta\omega^2 + \omega_r^2)}$. In this frame of reference, the dipolar Hamiltonian is rotated through angle θ by a time-independent unitary transformation $S(\theta) = \exp(i\theta I_y)$ to give

$$S^\dagger \mathcal{H}_1^0 S = \sum_{M,\alpha} G_M^\alpha = G .$$

The subscript M refers to the differences of magnetic quantum number of the I spins. The superscript $\alpha=1$, 2 and is the number of S spin operators in the Hamiltonian. The case $\alpha=0$ is understood, in order to make the notation consistent with our previous Paper I. The explicit forms for G_M are as follows:

$$G_0=\sum_{k>j} A_{jk}'\mathbf{I}_j\cdot\mathbf{I}_k+B_{jk}'I_{zj}I_{zk},$$

$$G_{\pm1}=\sum_{k>j} E_{jk}'(I_{zk}I_{\pm j}+I_{zj}I_{\pm k}),$$

$$G_{\pm2}=\sum_{k>j} D_{jk}'I_{\pm j}I_{\pm k},$$

$$G_0{}^2=\sum_{\beta>\alpha} a_{\alpha\beta}\mathbf{S}_\alpha\cdot\mathbf{S}_\beta+b_{\alpha\beta}S_{z\alpha}S_{z\beta},$$

$$G_{\pm1}{}^1=\sum_{k,\beta} C_{k\beta}'I_{\pm k}S_{z\beta},$$

$$G_0{}^1=\sum_{k,\beta} C_{k\beta}''I_{zk}S_{z\beta}.$$

The primed coefficients of the spin operators are given by

$$A_{jk}'=\tfrac{1}{2}A_{jk}(3\cos^2\theta-1),$$

$$B_{jk}'=\tfrac{1}{2}B_{jk}(3\cos^2\theta-1),$$

$$C_{k\beta}'=-\tfrac{1}{2}C_{k\beta}\sin\theta=-C_{k\beta}''\tan\theta,$$

$$D_{jk}'=\tfrac{1}{4}B_{jk}\sin^2\theta,$$

$$E_{jk}'=-\tfrac{1}{2}B_{jk}\sin\theta\cos\theta.$$

In order to integrate Eq. (40) we transform ρ and G to a reference frame rotating about I_z, i.e.,

$$\{\hat\rho,\hat G\}=\exp(i\omega_{\text{reff}}I_z t)\{\rho,G\}\exp(-i\omega_{\text{reff}}I_z t),$$

which then gives the new equation of motion

$$\frac{d\hat\rho}{dt}=-i[\hat G,\hat\rho]. \qquad (41)$$

This is integrated by a reiterative procedure to give a solution

$$\hat\rho(t,\tau)=\sum_n \hat\rho_n(t,\tau). \qquad (42)$$

Here τ allows for the evolution of the density matrix after the initial 90° rf pulse, just before the spin-locking pulse is applied. The nth term in the expansion Eq. (42) is given by

$$\hat\rho_n(t,\tau)=(-i)^n\int_0^t dt_1\cdots$$

$$\times\int_0^{t_{n-1}}[\hat G(t_1),[\cdots,[\hat G(t_n),\hat\rho(\tau)]\cdots]]_n dt_n. \qquad (43)$$

The subscript n and the dots denote an n-fold time-ordered commutation of $\hat G(t)$ with $\hat\rho(\tau)$.

1. Transient Response

The transient response during spin-locking is given by

$$\langle I_z\rangle=\sum_n\langle I_z\rangle_n=\sum_n \text{Tr}\{\hat\rho_n(t,\tau)I_z\}. \qquad (44)$$

As with the single-species case, it is necessary to carry the expansion of Eq. (44) to fourth order so as to introduce damping. For simplicity we take $\tau=0$. We note that the terms for odd n vanish in Eq. (44). The even terms are as follows:

Zeroth-order term. This is just the free-induction decay amplitude at $t=0$, i.e.,

$$\langle I_z\rangle_0=\text{Tr}\{\hat\rho_0(0)I_z\}, \qquad (45)$$

where $\hat\rho_0(0)=aI_z$. As in I, we exclude the dipolar part of the density matrix, thus assuming that the Zeeman temperature equilibration time is fast compared with the Zeeman-dipolar cross-relaxation time.

Second-order term. Integrating Eq. (43) for $n=2$ and substituting into Eq. (44) we obtain

$$\langle I_z\rangle_2=b\{[8(\cos2\omega_r t-1)/(2\omega_r)^2]A +[2(\cos\omega_r t-1)/\omega_r{}^2]A'\}, \qquad (46)$$

where $b=a\,\text{Tr}\{I_z{}^2\}$. In evaluating Eq. (46) and also the terms below we have used the fact that $\text{Tr}\{\prod_{\alpha,M}G_M{}^\alpha\}$ is zero unless $\sum_M M=0$.

Fourth-order term. We now turn to the evaluation of the fourth-order term. Again from Eqs. (43) and (44) we obtain after much algebra

$$\langle I_z\rangle_4=b\left[-4B\left(\frac{6(\cos2\omega_r t-1)}{(2\omega_r)^4}-\frac{t^2\cos2\omega_r t}{(2\omega_r)^2}+\frac{4t\sin2\omega_r t}{(2\omega_r)^3}\right)+4C\left(-\frac{4(\cos2\omega_r t-1)}{(2\omega_r)^4}-\frac{2t\sin2\omega_r t}{(2\omega_r)^3}\right)\right.$$

$$+D\left(\frac{4(\cos2\omega_r t-1)}{3\omega_r{}^4}-\frac{16(\cos\omega_r t-1)}{3\omega_r{}^4}\right)-E\left(\frac{6(\cos\omega_r t-1)}{\omega_r{}^4}-\frac{9(\cos2\omega_r t-1)}{\omega_r{}^4}+\frac{11t\sin\omega_r t}{\omega_r{}^3}-\frac{4t\sin2\omega_r t}{\omega_r{}^3}\right)$$

$$+F\left(\frac{2(\cos\omega_r t-1)}{\omega_r{}^4}+\frac{(\cos2\omega_r t-1)}{\omega_r{}^4}-\frac{5t\sin\omega_r t}{\omega_r{}^3}\right)+G\left(\frac{2(\cos\omega_r t-1)}{\omega_r{}^4}+\frac{(\cos2\omega_r t-1)}{\omega_r{}^4}+\frac{3t\sin\omega_r t}{\omega_r{}^3}\right)$$

$$\left.-B'\left(\frac{6(\cos\omega_r t-1)}{\omega_r{}^4}-\frac{t^2\cos\omega_r t}{\omega_r{}^2}+\frac{4t\sin\omega_r t}{\omega_r{}^3}\right)+C'\left(-\frac{4(\cos\omega_r t-1)}{\omega_r{}^4}-\frac{2t\sin\omega_r t}{\omega_r{}^3}\right)\right]. \qquad (47)$$

The constants appearing in Eqs. (46) and (47) are defined as follows:

$$A = \mathrm{Tr}\{G_2 G_{-2}\}/\mathrm{Tr}\{I_z^2\},$$

$$A' = \mathrm{Tr}\{G_1{}^1 G_{-1}{}^1\}/\mathrm{Tr}\{I_z^2\},$$

$$B = \mathrm{Tr}\{[G_0, G_2][G_0, G_{-2}]\}/\mathrm{Tr}\{I_z^2\},$$

$$B' = \mathrm{Tr}\{[(G_0 + G_0{}^2), G_1{}^1][(G_0 + G_0{}^2), G_{-1}{}^1]\}/\mathrm{Tr}\{I_z^2\},$$

$$C = \mathrm{Tr}\{[G_2, G_{-2}]^2\}/\mathrm{Tr}\{I_z^2\},$$

$$C' = \mathrm{Tr}\{[G_1{}^1, G_{-1}{}^1]^2\}/\mathrm{Tr}\{I_z^2\},$$

$$D = \mathrm{Tr}\{[G_1{}^1, G_{-1}{}^1][G_2, G_{-2}]\}/\mathrm{Tr}\{I_z^2\},$$

$$E = \mathrm{Tr}\{[G_1{}^1, G_{-2}][G_{-1}{}^1, G_2]\}\mathrm{Tr}\{I_z^2\},$$

$$F = \mathrm{Tr}\{[G_1{}^1, (G_0 + G_0{}^2)][G_1{}^1, G_{-2}]\}/\mathrm{Tr}\{I_z^2\},$$

$$G = \mathrm{Tr}\{[G_{-1}{}^1, (G_0 + G_0{}^2)][G_{-1}{}^1, G_2]\}/\mathrm{Tr}(I_z^2).$$

Adding all contributions and further simplifying our notation we obtain for Eq. (44) correct to $n=4$

$$\langle I_z \rangle = b \left\{ 1 - \Gamma_1 + \Gamma_1 \left[\left(1 + \frac{4Bt^2}{\Gamma_1(2\omega_r)^2} \right) \cos 2\omega_r t \right.\right.$$

$$\left. - 2\omega_r t \frac{\Gamma_2}{\Gamma_1} \sin 2\omega_r t + \cdots \right]$$

$$- \Gamma_1' + \Gamma_1' \left[\left(1 + \frac{B't^2}{\Gamma_1' \omega_r{}^2} \right) \cos \omega_r t \right.$$

$$\left.\left. - \omega_r t \frac{\Gamma_2'}{\Gamma_1'} \sin \omega_r t + \cdots \right] \right\}, \quad (48)$$

where

$$\Gamma_1 = 8A/(2\omega_r)^2 - (6B + 4C - 4D/3 - 9E - F - G)/\omega_r{}^4 + \cdots,$$

$$\Gamma_1' = 2A'/\omega_r{}^2 - (6B' + 4C' + 16D/3 + 6E - 2F - 2G)/\omega_r{}^4 + \cdots,$$

$$\Gamma_2 = (16B + 8C + 4E)/(2\omega_r)^4 + \cdots,$$

$$\Gamma_2' = (-11E + 5F + 4B' - 3G + 2C')/\omega_r{}^4 + \cdots.$$

2. Gaussian Damping Approximation

Just as in the single-ingredient spin system, we may contract the trigonometric expression in Eq. (48) to give

$$\langle I_z \rangle \simeq b\{ 1 - \Gamma_1 + \Gamma_1 (\cos 2\omega_r t (1 + \Gamma_2/\Gamma_1)$$
$$+ [4Bt^2/(2\omega_r)^2 \Gamma_1] \cos 2\omega_r t + \cdots)$$
$$- \Gamma_1' + \Gamma_1' (\cos \omega_r t (1 + \Gamma_2'/\Gamma_1')$$
$$+ [B't^2/\omega_r{}^2 \Gamma_1'] \cos \omega_r t + \cdots) \}. \quad (49)$$

This is valid if

$$2\omega_r \Gamma_2 t/\Gamma_1 \ll 1 \quad (50a)$$

and

$$\omega_r \Gamma_2' t/\Gamma_1' \ll 1. \quad (50b)$$

Following the procedure in I, we take the B and B' terms in Eq. (49) as being the first of a damped func-
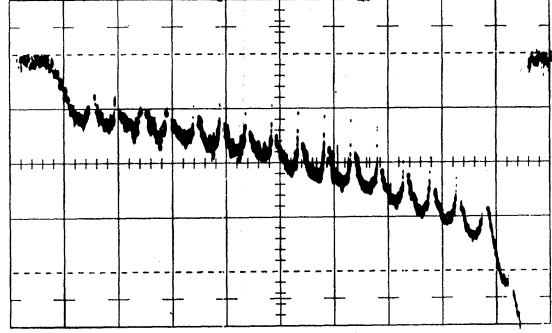

FIG. 1. Photograph of positively detected solid-echo chain from Na^{23} in a single crystal of NaF with its [110] axis along $\mathbf{H}_0$. Notice the sharp initial decrease in signal and the rather poorly formed first echo. (See Ref. 18 for a discussion of this.) $\tau = 50\ \mu$sec and the time-base sweep is 0.2 msec/large div.

tion which we assume to be Gaussian in both cases. We are thus able to write Eq. (49) in approximate but closed form giving finally

$$\langle I_z \rangle \simeq b\{ 1 - \Gamma_1 + \Gamma_1 \exp[4Bt^2/(2\omega_r)^2 \Gamma_1] \cos 2\omega_r t (1 + \Gamma_2/\Gamma_1)$$
$$- \Gamma_1' + \Gamma_1' \exp[B't^2/\omega_r{}^2 \Gamma_1'] \cos \omega_r t (1 + \Gamma_2'/\Gamma_1') \}. \quad (51)$$

When expanded in powers of time this agrees with the exact expansion up to t^2. Both the inequalities, Eqs. (50a) and (50b) are satisfied over the range of interest for the experiments presented, i.e., for spin-locking fields greater than the local field and times of the order of a few T_2. Truncation of Γ_1, etc. is justified for high fields.

III. EXPERIMENTAL RESULTS AND DISCUSSION

A. Multiple-Pulse Experiments

Multiple-pulse sequences of the type $90°\text{-}\tau\text{-}90°_{90°}\text{-}(2\tau\text{-}90°_{90°})_{N-1}$ have been applied at 9.0 MHz to the Na^{23} nuclei and to the F^{19} nuclei in a single crystal of NaF, as well as the F^{19} nuclei in doped single crystals of CaF_2. The external static magnetic field $\mathbf{H}_0$ was adjusted in each case for exact resonance. The apparatus details are the same as in I. The sodium fluoride crystal was obtained from Harshaw Chemicals Inc. The doped caclium fluoride samples were machined cylinders with their cylindrical axes along the [110] direction. These were obtained from Optovac Inc.[19]

Alignment of the crystal axes was attained by attaching the crystals to a simple goniometer and observing the complete rotation pattern of the free-induction decay. By this method, alignment was judged to be correct to better than 1°.

1. Experiments on NaF

These experiments were performed at 298°K. At this temperature $T_1(Na^{23}) = 11.5$ sec and $T_1(F^{19}) = 19.0$ sec.
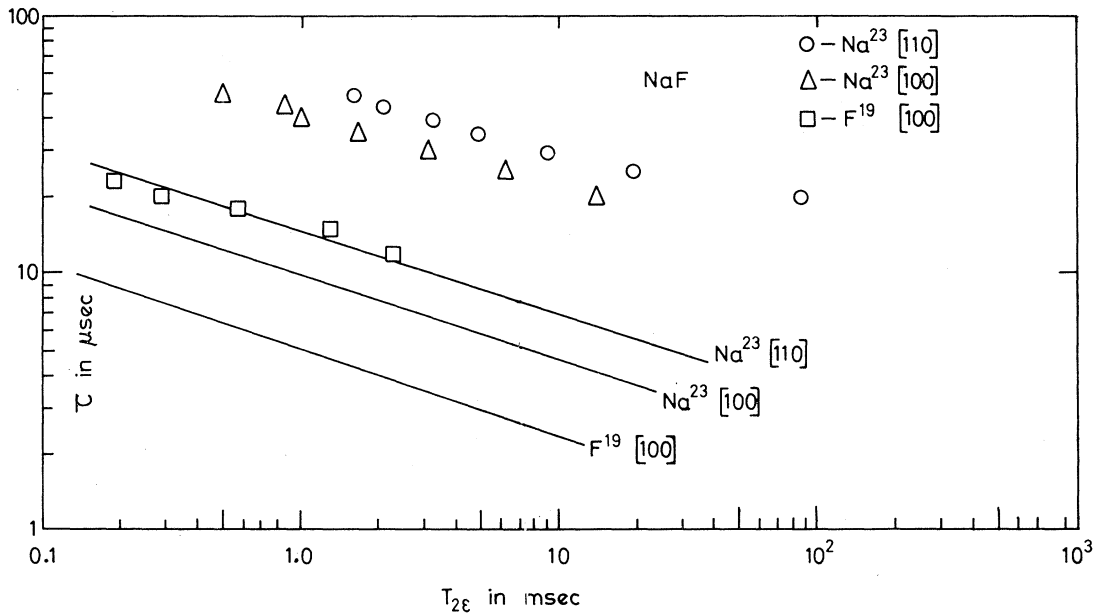
FIG. 2. Log-log graph of $T_{2\epsilon}$ versus τ for Na^{23} and F^{19} in a crystal of NaF. The circles, etc., are experimental data for H_0 along the crystal axes shown. The solid lines are the theoretical expression Eq. (16).

No anisotropy in the spin-lattice relaxation time was observed for either nucleus.

As in the case of a single magnetic ingredient, the effect of applying multiple-pulse trains to either Na^{23} or F^{19} spins is to prolong the free induction decay by orders of magnitude for $\tau < T_2$. An important difference between the decay train in a single-ingredient sample and that of two equally abundant species, is that in the former the decay-train envelope approximates quite well to an exponential function, whereas for Na^{23} spins in NaF, the decay-train envelope is clearly nonexponential, Fig. 1. The rather sharp drop in signal amplitude that occurs during the first two echoes, persists to varying extent for all τ. It is thus clear experimentally why reiteration of the loss in echo intensity of the fourth echo in each cycle, or the attenuated diagonal density matrix assumption must fail when projecting the decay train for long times. After the second echo, the echo chain settles down to a reasonably good exponential decay, the time constant $(T_{2\epsilon})$ of which has been measured as a function of τ and crystal orientation. We have also measured $T_{2\epsilon}$ for F^{19} in NaF with H_0 along the [100] axis. These experimental results together with the naive theoretical expression, Eq. (16) are plotted in Fig. 2. The predicted amplitudes of $T_{2\epsilon}$ are all about two orders of magnitude too small. A further disconcerting feature is that the experimental data are fitted by a τ^{-x} dependence with $x = 3.5$–4.0. The theoretical value of τ which makes the fourth echo amplitude greater than the first three echoes is obtained from the intersection of the theoretical curve in Fig. 4(a) with the theoretical curves in Fig. 4(b) and Figs. 3(a) and 3(b). This gives a value of $\tau = 10$ μsec. How-

ever, the intersection of the curve $T_{2\epsilon} = 8/M_{4\epsilon}{}^4\tau^3$ with the corresponding experimental data in Fig. 2 occurs for $\tau \gg 10$ μsec. Thus the limiting behavior of $T_{2\epsilon}$ for $\tau \to 0$ does not converge to the naive theoretical expression.

The 90° pulse width for the sodium spins in these experiments was 4.0 μsec. To test the effect of finite pulse width, the Na^{23}[110] data in Fig. 2 was repeated using a 9.0-μsec pulse. The effect was to decrease the values of $T_{2\epsilon}$ by about 25% and also to increase the gradient slightly. We therefore eliminate the finiteness of the pulse width as a possible explanation of the deviation of our results from the elementary theory.

In order to try to understand the large discrepancy in magnitude between theory and experiment, the amplitudes of the first four echoes in Na^{23} have been measured as a function of τ for H_0 along [110]. The normalized results together with the theoretical expressions Eqs. (9)–(15) are plotted in Figs. 3 and 4. Good agreement with theory is obtained for the first- and second-echo amplitude for $\tau \leq 50$ μsec. Good agreement with theory for $\tau \leq 40$ μsec is also obtained for the third echo if a fourth-order term is added in Eq. (11). Though we have theoretical expressions for $M_{4\epsilon}{}^3$, these are more formidable to evaluate than $M_{4\epsilon}{}^4$, so we have chosen to fit Fig. 4(b) empirically. This requires that $M_\epsilon{}^3 = -0.664 \times 10^{17}$ rad^4 sec^{-1}.

In contrast to the first three echoes, the variation of the fourth echo amplitude with τ is not described very well by Eq. (12). The best empirical fit of a sixth-order term with $M_{6\epsilon}{}^4 = 5.0 \times 10^{27}$ rad^6 sec^{-6} causes the theoretical curve to diverge at $\tau = 15$ μsec. It is clear that only by going to very high order in τ can one hope to

describe the variation of fourth-echo amplitude with τ for up to 50 μsec.

An interesting semiempirical fact is that iteration of the loss in amplitude between the first and third echoes gives a much better fit to $T_{2\epsilon}$. However, since this procedure is not based on the realization of the full symmetry properties of the complete dipolar Hamiltonian, we do not pursue the matter here.

2. Experiments on Doped CaF₂

Experiments have been performed on the F^{19} spins in doped CaF_2 with $\mathbf{H}_0$ along the [111] direction. In the first case, the dopant was 0.1% $Sm^{2+,3+}$. $T_{2\epsilon}$ was measured as a function of τ at 296 and 78°K and in both cases, over the range studied, there is little difference between these values and $T_{2\epsilon}$ in pure CaF_2, Fig. 5. The measured spin-lattice relaxation times of F^{19} for this sample were $T_1 = 397$ msec (298°K); $T_1 = 75.5$ msec
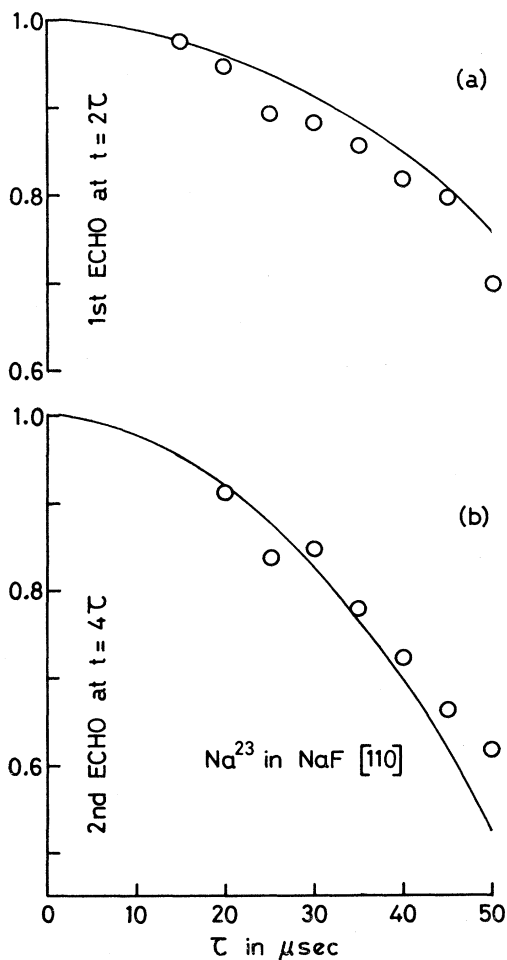

FIG. 3. Experimental solid-echo amplitudes (circles) for Na²³ in NaF with $\mathbf{H}_0$ along the [110] axis. (a) Normalized first-echo amplitude at $t = 2\tau$ versus τ. The solid line is the theoretical expression, Eq. (9b). (b) Normalized second-echo amplitude at $t = 4\tau$ versus τ. The solid line is the theoretical curve Eq. (10).
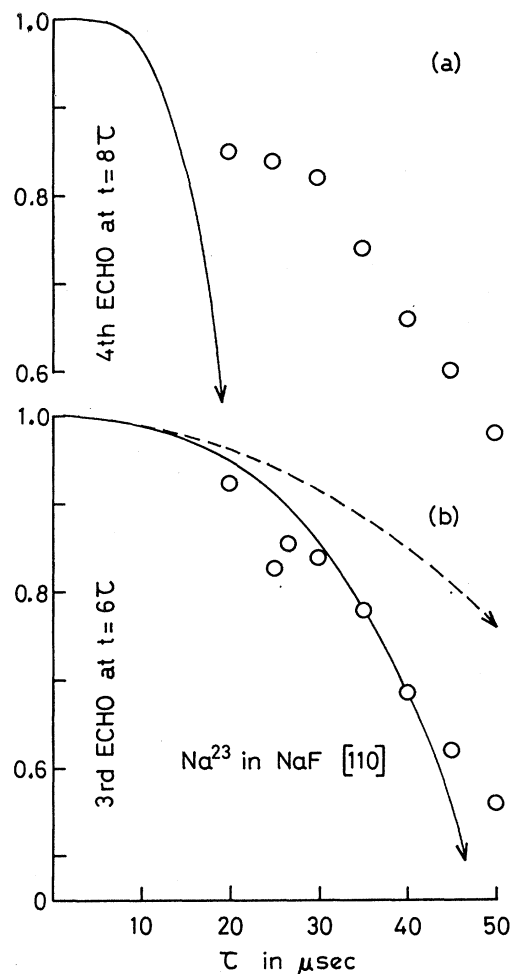

FIG. 4. Experimental solid-echo amplitudes (circles) for Na²³ in NaF with $\mathbf{H}_0$ along the [110] axis. (a) Normalized fourth-echo amplitude at $t = 8\tau$ versus τ. The solid line is the theoretical expression, Eq. (14). (b) Normalized third-echo amplitudes at $t = 6\tau$ versus τ. The broken line corresponds to the first two terms in Eq. (11), the solid line includes all three terms. The value of $M_{4\epsilon}{}^3$ was chosen for best empirical fit.

(78°K). Thus over the range of τ used, T_1 does not seem to be affecting $T_{2\epsilon}$.

In the second case, the dopant was 0.1% U^{3+}. Here the data at 78°K seem to have values of $T_{2\epsilon}$ consistently shorter than those measured at 295°K. The measured spin-lattice relaxation times of F^{19} in this sample were $T_1 = 1.12$ msec (295°K); $T_1 = 0.59$ msec (78°K). From Fig. 5, we see that there is no significant difference between the slope of the experimental data and the theoretical curve for the pure material. Note that although it might be more to the point to measure the spin-lattice relaxation time in the rotating reference frame $(T_{1\rho})$, in the present examples, we would not expect much difference between T_1 and $T_{1\rho}$.

We were hoping that at the lower temperature (78°K) the relaxation rate of the paramagnetic ion would be slowed down sufficiently so that the electron dipolar
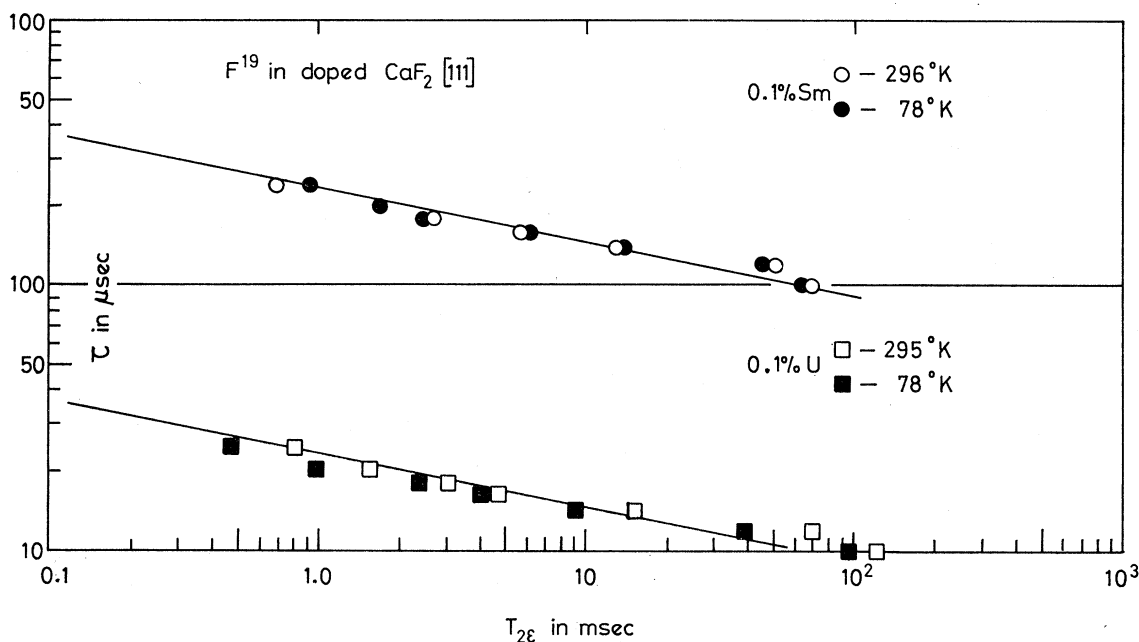
FIG. 5. Log-log graph of $T_{2\epsilon}$ versus τ for F^{19} in a single crystal of doped CaF_2. The solid lines correspond to the theoretical expression in the case of a pure sample [see Eq. (20) of Ref. 2].

field around an impurity would have a nonzero time average at the near-neighbor F^{19} sites. Equipment limitations prevented our going to lower temperatures. Since any deviation in solid-echo amplitude from that of the pure material is effectively *amplified* in long multiple-pulse trains, we feel that this technique could yield useful results thus complementing other indirect methods of studying paramagnetic impurities in solids.

B. Multiple-Pulse Double-Resonance Experiments

Double-resonance experiments have been performed between the sodium and fluorine spins in NaF with H_0 along the [100] axis. These experiments were reported briefly in our earlier paper.[13] The Na^{23} spins were pulsed at 9.0 MHz by a $90°-\tau-90°_{90°}-(2\tau-90°_{90°})_{N-1}$ sequence at resonance and with $\tau = 25$ μsec. The 90° rf pulse width was 4.5 μsec, corresponding to a peak rf pulse field $H_{pNa} = 50$ G. A sustained echo chain lasting for 4.5 msec was thus produced, Fig. 6(a). The same experiment was repeated, but with the F^{19} nuclei simultaneously irradiated at their Larmor frequency (approximately 32.0 MHz) by an rf field with rotating component $H_{rF} = 8.8$ G for a duration $t_{wF} = 2.0$ msec, Fig. 6(b). This caused almost complete destruction of the Na^{23} echo signal.

The coil producing the F^{19} rf field was a short circular solenoid, its axis coinciding with that of the receiver coil. The Na^{23} rf field coil geometry was as used in all the other experiments, i.e., a cylindrical Helmholtz configuration following the design of Lurie and Slichter[15] but allowing easy removal of the sample. The particular coil geometry chosen, while minimizing the coupling

between the two transmitter coils, offers maximum coupling between the F^{19} transmitter coil and the receiver coil. Although the receiver coil was tuned to 9.0 MHz, there was still sufficient rf power absorbed by it at 32.0 MHz to completely blank out the echo signal and noise while the fluorine spins were being irradiated.

Higher values of H_{rF} produced less destruction of the echo train amplitude for constant t_{wF}. This is due to the slower cross-relaxation time. For $H_{rF} = 25.6$ G an increase in amplitude of the echo train was observed following the fluorine irradiation pulse. We attribute this effect to the partial removal of the dipolar cross-coupling term by the action of high fluorine stirring field. This is similar to the work of Sarles and Cotts[20] and has been discussed briefly in our earlier paper.[13] Here we restrict ourselves to discussing the destructive double-resonance effects.

In the pulsed double-resonance experiments of Hahn and Hartmann[14] and of Lurie and Slichter,[15] the destruction of spin-locked A magnetization is brought about by an energy conserving cross relaxation between the two simultaneously irradiated spin species, both of which are regarded as independent thermal reservoirs, A and B. When the two reservoirs have reached a common spin temperature no further net changes in magnetization occur. The approach to equilibrium will be fastest when the spin energy level differences of both species in their respective rf fields, are made equal, i.e., when the Hahn condition $\gamma_A H_{rA} = \gamma_B H_{rB}$ is satisfied. The ratio of the initial to final spin-locked magnetiza-

[20] L. R. Sarles and R. M. Cotts, Phys. Rev. 111, 853 (1958).

tion is then given by

$$M_f/M_i = 1/(1+\epsilon),$$

where $\epsilon = C_B H_{rB}^2/C_A(H_{rA}^2 + H_L^2)$. The nuclear Curie constant is given by $C_I = N_I \gamma_I^2 \hbar^2 I(I+1)/3k$, where N_I is the number of nuclei. H_L is the local field[15] which for Na^{23} in NaF with $\mathbf{H}_0$ along [100] is $H_L = 4.1$ G.

In our experiments, we do not have a normal spin-locked A system. The destruction of signal which occurs in these experiments is, therefore, open to at least two interpretations: (a) cross relaxation under the action of H_{pNa} in the finite duration of the 90° pulses; (b) cross relaxation under the action of a mean pulse field $\bar{H}_{pNa}$. In case (a) with $H_{pNa} = 50$ G and $H_{rF} = 8.8$ G, the maximum fractional destruction of magnetization is $M_f/M_i = 1/1.08$. In case (b) with $\bar{H}_{pNa} = 4.5$ G and $H_{rF} = 8.8$ G, the maximum fractional destruction of magnetization is $M_f/M_i = 1/6.26$, which is in much better agreement with the experimental results shown in Fig. 6.

C. Long-Pulse Experiments

Long-pulse spin-locking experiments following at time τ an initial 90° rf pulse, have been performed on the sodium spins in NaF at exact resonance. The experimental details are similar to the single-species experiments described in I. All data are taken with $\mathbf{H}_0$ along the [100] direction.

For fixed spin-locking field H_r, the magnetization is found to oscillate as a function of the spin-locking time t_{wr}, damping out to a quasiequilibrium value in about 200 μsec. Experimental data for $H_r = 6.5$, 4.0, and 2.0 G are shown in Fig. 7(b) together with the theoretical expression, Eq. (51), plotted for $H_r = 6.5$ G only. Comparison with theory for 4.0 and 2.0 G is impossible, since $\langle I_z \rangle = 1 - \Gamma_1 - \Gamma_1'$ goes negative in this region due to the truncation. Figure 7(a) shows Eq. (51) plotted
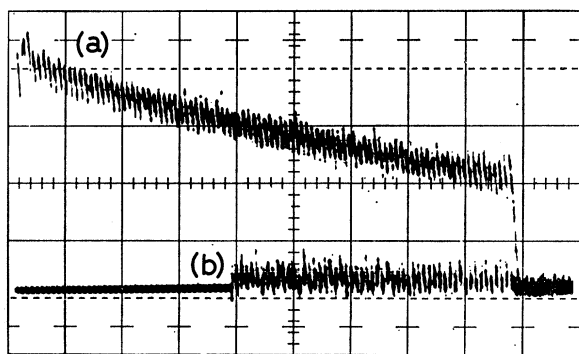

FIG. 6. Doubly exposed photograph of the positively detected solid-echo trains of the Na^{23} resonance in a single crystal of NaF. The static field $\mathbf{H}_0$ is along the [100] direction, $\tau = 25$ μsec for both traces and the time-base sweep is 0.5 msec/large div. (a) Solid-echo train with no irradiation of the F^{19} spins. (b) Echo train following F^{19} irradiation for 2.0 msec and rotating field component $H_{rF} = 8.8$ G. This shows an initial blanking of the receiver with consequent loss of both signal and noise. This is followed by inspection of the remaining signal, which is almost completely destroyed in this sequence.
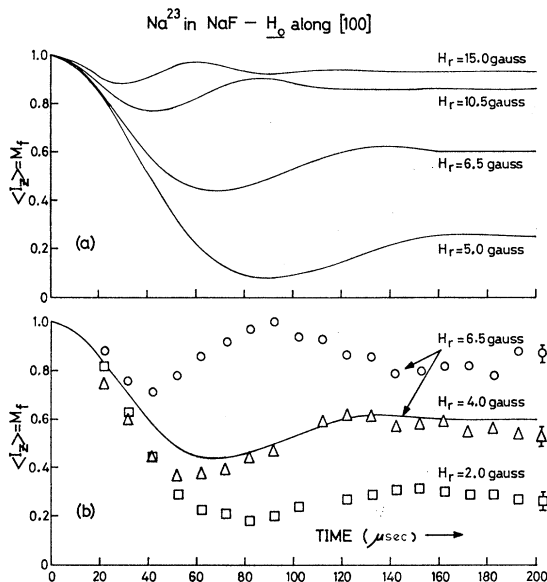

FIG. 7. Spin-locked magnetization versus t_{wr} for Na^{23} in NaF with $\mathbf{H}_0$ along the [100] direction. (a) Theoretical expression Eq. (51) plotted for various values of H_r. (b) Experimental data for $H_r = 6.5$, 4.0, and 2.0 G. The solid line is Eq. (51) for $H_r = 6.5$ G.

for various values of H_r and with $\mathbf{H}_0$ along the [100] direction.

The agreement with theory for the 6.5-G data is not too good since Γ_1 and Γ_1' are beginning to diverge quite severely at this field. In Eq. (51) the $\cos 2\omega_r t(1+\Gamma_1/\Gamma_2)$ term is damped out rapidly, the period of the oscillations being dominated by the fundamental angular frequency $\omega_r(1+\Gamma_2'/\Gamma_1')$. Experiments confirm that there is no apparent second harmonic content in the oscillations.

The theory presented becomes more valid for high H_r, but unfortunately high-field oscillation data are not available. However, the intermediate field case, $H_r = 6.5$ G, is sufficient to substantiate the gross features of the theory.

D. Equilibrium Magnetization

The rapid spin-locking procedure is a constant energy process ($\Delta E = 0$) in which the magnetic energy of the spin system is conserved. This is discussed in more detail in I and predicts a final spin-locked thermal-equilibrium magnetization M_f, when all transients due to dipolar-Zeeman mutual exchange and cross-relaxation processes have decayed away, given by

$$M_f = \frac{M_0(H_r^2 + H_r H_L^2/H_0)}{H_r^2 + H_L^2} \simeq \frac{M_0 H_r^2}{H_r^2 + H_L^2},$$

where M_0 is the initial thermal-equilibrium magnetization. For a two-ingredient spin system, the local field H_L is given by[15]

$$H_L^2 = \tfrac{1}{3}M_{2II} + M_{2IS} + \tfrac{1}{3}M_{2SS}\gamma_S^2 N_S S(S+1)/$$
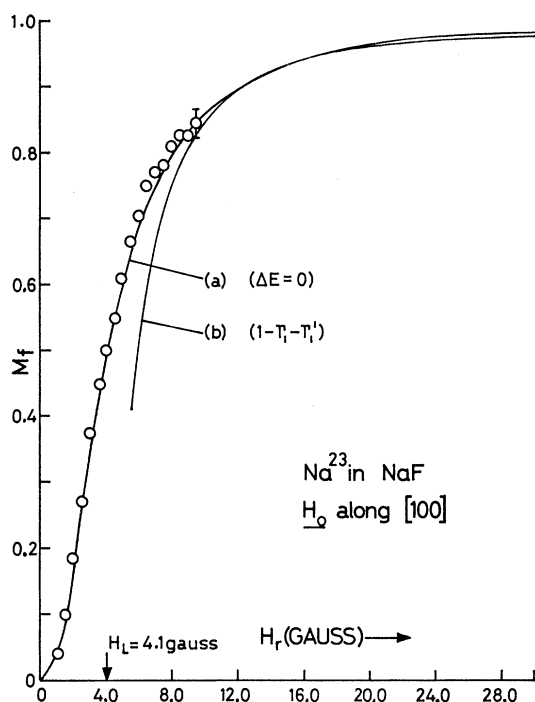$$\gamma_I^2 N_I I(I+1),$$

FIG. 8. Spin-locked Na^{23} magnetization versus magnetic field H_r for t_{wr} fixed at 10 msec. The solid curve (a) is the theoretical final thermal-equilibrium value. Curve (b) is the theoretical quasi-equilibrium time-independent part of Eq. (51).

where M_{2ab} is the contribution (in G^2) of the b spins to the second moment of the a-spin absorption line.

Long-pulse spin-locking experiments were performed with t_{wr} held at 10 msec and H_r varied from 1.0 up to 9.5 G. The experimental data are plotted in Fig. 8. These are compared with the theoretical expression for the thermal-equilibrium magnetization. We see that good agreement is obtained between theory [solid curve (a), Fig. 8] and the data over the range studied. For higher H_r one might expect a long dipolar-Zeeman cross-relaxation time, thus preventing temperature equilibration of the Zeeman and dipolar energy reservoirs in 10 msec. In this case, the quasiequilibrium Zeeman magnetization following establishment of the Zeeman spin temperature would be predicted by the time-independent part of Eq. (51), i.e., $\langle I_z \rangle = 1 - \Gamma_1 - \Gamma_1'$. This expression is also plotted [curve (b), Fig. 8], and unlike the single-ingredient case, begins to diverge for $H_r \lesssim 3H_L$. Above $3H_L$, where the quasiequilibrium theory is valid, the difference between curves (a) and (b) in Fig. 8 is negligible, thus making observation of cross relaxation impossible.

IV. CONCLUSIONS

For a spin system comprising two abundant species only one of which is irradiated at resonance, we have shown that iteration of the loss in amplitude of the fourth echo in a coherent multiple-pulse experiment cannot be used to predict the over-all time constant $T_{2\epsilon}$ of the echo train decay envelope. Experiments on F^{19} and Na^{23} in a single crystal of NaF confirm this.

A new theoretical treatment of the multiple-pulse experiments based on a logarithmic operator formalism shows that for the fourth echo the leading error term in the usual time expansion, which is correct to fourth order in time, in fact, vanishes identically when taken to all orders in the perturbation expansion. A different method of projecting to long times, the short time behavior of the echo train, is discussed, and the analogy made between the effective line narrowing produced by multiple-pulse sequences and spectral line narrowing in solids due to the presence of an exchange interaction. Using this model, which describes the short-time behavior as well as the long-time characteristics of the echo train, an expression for $T_{2\epsilon}$ is derived which has the right τ dependence.

As with the single-ingredient spin system, there is a small oscillation of the echo amplitudes. Theoretical examination of the first four echoes shows that for short times, the amplitude of the second echo should be lowest and the fourth echo highest. Simulation of this situation by spin locking in a long-pulse rf field corresponding to the mean field of the short 90° pulses, shows the spin-locked magnetization to oscillate. For high fields, calculation shows that the period of the oscillations is $2\pi/\gamma_I H_r$. The terms in the theory giving a second harmonic contribution to the oscillations are rapidly damped in time. If H_r is replaced by the mean pulse field $\bar{H}_r = \pi/4\gamma_I\tau$ then the period 8τ corresponds precisely with that expected on symmetry grounds in the mutliple-pulse experiments.

Some multiple-pulse experiments have been performed on the F^{19} nuclei in paramagnetically doped CaF_2 in the temperature range 295–78°K. Since the dependence of $T_{2\epsilon}$ on τ does not change significantly from that of the undoped material over this range, the time average of the electron-nuclear dipolar interaction is effectively zero.

Pulsed double-resonance experiments performed on the Na^{23} and F^{19} nuclei in NaF show that cross-relaxation can take place with spins partially spin-locked by an in-phase multiple-pulse sequence.

ACKNOWLEDGMENTS

APPENDIX: EVALUATION OF TRACE PRODUCTS AND LATTICE SUMS

In this Appendix we wish to evaluate the various traces occurring in Sec. II.

Multiple-pulse experiments. As noted in the text,

$$[[U_2{}^1]] = M_{2\epsilon}{}^1 = -\tfrac{1}{2}M_{2\epsilon}{}^2 = -M_{2\epsilon}{}^3$$

$$= [\tfrac{1}{3}S(S+1)/N_I] \sum_{k,\beta} C_{k\beta}{}^2 .$$

In order to evaluate both $M_{4\epsilon}{}^3$ and $M_{4\epsilon}{}^4$ the following commutators are required:

$$FEI_x = -FE'I_x$$

$$= -i^2 \sum_\beta \sum_{k>j} B_{jk}(C_{j\beta}I_{xj}I_{zk} + C_{k\beta}I_{xk}I_{zj})S_{z\beta} ,$$

$$F'EI_x = -F'E'I_x$$

$$= i^2 \sum_\beta \sum_{k>j} B_{jk}(C_{j\beta}I_{yk}I_{xj} + C_{k\beta}I_{yj}I_{xk})S_{z\beta} ,$$

$$\left.\begin{matrix} EF \\ E'F' \end{matrix}\right\} I_x = i^2 \sum_\delta \sum_{k>j} A_{jk}(C_{j\delta} - C_{k\delta})\left(\left\{\begin{matrix} I_{zj} \\ I_{yj} \end{matrix}\right\} - \left\{\begin{matrix} I_{zk} \\ I_{yk} \end{matrix}\right\}\right)$$

$$\times I_{xk}S_{z\delta} - B_{jk}C_{k\delta}\left(\left\{\begin{matrix} I_{zj} \\ I_{yj} \end{matrix}\right\} + \left\{\begin{matrix} I_{zk} \\ I_{yk} \end{matrix}\right\}\right)I_{xj}S_{z\delta} ,$$

$$F^2 I_x = -F'^2 I_x$$

$$= -i^2\left(\sum_{k,\beta} C_{k\beta}{}^2 I_{xk}S_{z\beta}{}^2 \right.$$

$$\left. + \sum_k \sum_{\beta>\alpha} C_{k\alpha}C_{k\beta}I_{xk}S_{z\alpha}S_{z\beta}\right) ,$$

$$FF'I_x = F'FI_x = 0 ,$$

$$S\left\{\begin{matrix} P \\ Q \end{matrix}\right\} I_x = G\left\{\begin{matrix} F \\ F' \end{matrix}\right\} I_x$$

$$= -i^2 \sum_m \sum_{\beta>\alpha} a_{\alpha\beta}(C_{m\alpha} - C_{m\beta})$$

$$\times (S_{y\alpha}S_{x\beta} - S_{x\alpha}S_{y\beta})\left\{\begin{matrix} I_{ym} \\ I_{zm} \end{matrix}\right\} .$$

Multiplying the various commutators together and summing over all subscripts we obtain the following traces:

$$[[EFEF]] = \sum_\delta \sum_{k>j} [A_{jk}B_{jk}(C_{j\delta} - C_{k\delta})^2$$

$$+ B_{jk}{}^2(C_{j\delta}{}^2 + C_{k\delta}{}^2)]\tfrac{1}{9}I(I+1)S(S+1) ,$$

$$[[FE^2F]] = \sum_\delta \sum_{k>j} [2A_{jk}{}^2(C_{j\delta} - C_{k\delta})^2$$

$$+ 2B_{jk}{}^2(C_{j\delta}{}^2 + C_{k\delta}{}^2)]\tfrac{1}{9}I(I+1)S(S+1) ,$$

$$[[EF^2E]] = \sum_\beta \sum_{k>j} B_{jk}{}^2(C_{j\beta}{}^2 + C_{k\beta}{}^2)\tfrac{1}{9}I(I+1)S(S+1) ,$$

$$[[FE'EF]] = \sum_\delta \sum_{k>j} (C_{j\delta} - C_{k\delta})^2(2A_{jk}{}^2 + A_{jk}B_{jk})$$

$$\times \tfrac{1}{9}I(I+1)S(S+1) ,$$

$$[[FE'^2F]] = \sum_\delta \sum_{k>j} 2A_{jk}{}^2(C_{j\delta} - C_{k\delta})^2 \tfrac{21}{9}I(I+1)S(S+1) ,$$

TABLE I. Lattice sums in inverse Å units for NaF with the static field along the principal crystal axes. The values computed are the spatial and angular sums, i.e., $P_{jk} = 2P_2(\cos\theta_{jk})/r_{jk}{}^3$. The first two sums include an integrated contribution taken from the twenty-first shell.

	[100]	[110]	[111]
$\sum_k P_{jk}{}^2$	7.087×10^{-3}	1.012×10^{-2}	1.113×10^{-2}
$\sum_\alpha P_{j\alpha}{}^2$	8.084×10^{-2}	2.322×10^{-2}	4.014×10^{-3}
$\sum_k P_{jk}{}^4$	3.439×10^{-6}	2.309×10^{-5}	8.174×10^{-5}
$\sum_{k,l} P_{jk}{}^2 P_{jl}P_{kl}$	1.063×10^{-5}	8.475×10^{-6}	1.700×10^{-5}
$\sum_\alpha P_{j\alpha}{}^4$	1.560×10^{-3}	9.805×10^{-5}	2.006×10^{-6}
$\sum_{k,\alpha} P_{jk}{}^2 P_{j\alpha}{}^2$	5.645×10^{-4}	2.317×10^{-4}	4.304×10^{-5}
$\sum_{k,\alpha} P_{jk}{}^2 P_{j\alpha}P_{k\alpha}$	3.945×10^{-5}	1.994×10^{-5}	1.249×10^{-5}
$\sum_{k,\alpha} P_{jk}{}^2 (P_{j\alpha} - P_{k\alpha})^2$	1.047×10^{-3}	4.222×10^{-4}	6.030×10^{-5}
$\sum_{k,\alpha} P_{j\alpha}{}^2 P_{k\alpha}{}^2$	4.954×10^{-3}	4.349×10^{-4}	1.269×10^{-5}

$$[[F^4]] = \sum_{k,\beta} C_{k\beta}{}^4 \tfrac{1}{5}[I^2(I+1)^2 - \tfrac{1}{3}I(I+1)]$$

$$+ \sum_k \sum_{\alpha>\beta} 2C_{k\alpha}{}^2 C_{k\beta}{}^2 \tfrac{1}{9}S^2(S+1)^2 ,$$

$$[[FG^2F]] = \sum_m \sum_{\beta>\alpha} 2a_{\alpha\beta}{}^2(C_{m\alpha} - C_{m\beta})^2 \tfrac{1}{9}S^2(S+1)^2 ,$$

$$[[F'^2F^2]] = -\sum_{k,\beta} C_{k\beta}{}^4 \tfrac{1}{5}[I^2(I+1)^2 - \tfrac{1}{3}I(I+1)]$$

$$+ \sum_k \sum_{\beta>\alpha} 2C_{k\alpha}{}^2 C_{k\beta}{}^2 \tfrac{1}{9}S^2(S+1)^2 ,$$

$$[[EF'EF']] = -\sum_\delta \sum_{k>j} A_{jk}B_{jk}(C_{j\delta} - C_{k\delta})^2$$

$$\times \tfrac{1}{9}I(I+1)S(S+1) .$$

Carrying through the substitution in Eq. (15), we obtain

$$M_{4\epsilon}{}^4 = \frac{-8}{N_I}\{\sum_j \sum_{\beta>\alpha} 8a_{\alpha\beta}{}^2(C_{j\alpha} - C_{j\beta})^2 \tfrac{1}{9}S^2(S+1)^2$$

$$+ \sum_\alpha \sum_{k>j} [8A_{jk}{}^2(C_{j\alpha} - C_{k\alpha})^2 + 2A_{jk}B_{jk}(C_{j\alpha} - C_{k\alpha})^2$$

$$+ B_{jk}{}^2(C_{j\alpha}{}^2 + C_{k\alpha}{}^2)]\tfrac{1}{9}I(I+1)S(S+1)\} .$$

A similar expression may be obtained for $M_{4\epsilon}{}^3$ using the above evaluated averages.

Long-pulse experiments. The evaluation of terms A, B, and C have been discussed previously in I. We quote the results for convenience only:

$$A = \frac{3}{8N_I} \sum_{j\neq k} A_{jk}{}^2 I(I+1) ,$$

TABLE II. Computed values of quantities defined in Sec. II.

Resonant species Na	F	[100]	[110]	[111]
$M_{2\epsilon}{}^1$(rad^2 sec^{-2})		$\cdots$	9.50×10^7	$\cdots$
$M_{4\epsilon}{}^4$(rad^4 sec^{-4})		-8.38×10^{18}	-3.35×10^{18}	-4.90×10^{17}
	$M_{4\epsilon}{}^4$(rad^4 sec^{-4})	-5.89×10^{19}	$\cdots$	$\cdots$
H_L(G)		4.1		
A (rad^2 sec^{-2})		$7.00\pi^2\times10^5$		
A'(rad^2 sec^{-2})		$3.56\pi^2\times10^7$		
B(rad^4 sec^{-4})		$-1.73\pi^4\times10^{12}$		
B'(rad^4 sec^{-4})		$-1.33\pi^4\times10^{15}$		
C(rad^4 sec^{-4})		$1.97\pi^4\times10^{13}$		
C'(rad^4 sec^{-4})		$1.27\pi^4\times10^{15}$		
D(rad^4 sec^{-4})		$3.08\pi^4\times10^{12}$		
E(rad^4 sec^{-4})		$-1.23\pi^4\times10^{12}$		
F(rad^4 sec^{-4})		$4.70\pi^4\times10^{12}$		
G(rad^4 sec^{-4})		$4.70\pi^4\times10^{12}$		

$$B=-(9/32N_I)\sum_{k\neq j} A_{jk}{}^4[(12I(I+1)+1)/15-\tfrac{2}{3}],$$

$$-(9/24N_I)\sum_{l\neq k\neq j}(A_{kl}{}^2A_{jk}{}^2+2A_{jk}{}^2A_{jl}A_{kl})I^2(I+1)^2,$$

$$C=(27/64N_I)\sum_{k\neq j}A_{jk}{}^4\{4(2I^2+2I+1)/5-1\}I(I+1)$$

$$+(9/24N_I)\sum_{l\neq k\neq j}A_{jk}{}^2A_{kl}{}^2I^2(I+1)^2.$$

To evaluate the remaining terms we require the following commutators:

$$[G_0,G_{\pm1}{}^1]=\sum_\beta\sum_{k>j}\{jk\beta\}_\pm+\{kj\beta\}_\pm,$$

where

$$\{jk\beta\}_\pm=\pm(A_{jk}{}'+B_{jk}{}')C_{k\beta}{}'I_{zj}I_{\pm k}S_{z\beta}$$

$$\mp A_{jk}{}'C_{k\beta}{}'I_{\pm j}I_{zk}S_{z\beta},$$

$$[G_0{}^2,G_{\pm1}{}^1]=\sum_k\sum_{\beta>\alpha}\{\alpha\beta k\}_\pm+\{\beta\alpha k\}_\pm,$$

where

$$\{\alpha\beta k\}_\pm=\tfrac{1}{2}a_{\alpha\beta}C_{k\beta}{}'(S_{+\alpha}S_{-\beta}-S_{-\alpha}S_{+\beta})I_{\pm k},$$

$$[G_{+1}{}^1,G_{-1}{}^1]=\sum_{k,\beta}2C_{k\beta}{}'^2I_{zk}S_{z\beta}{}^2$$

$$+\sum_k\sum_{\beta>\alpha}2C_{k\alpha}{}'C_{k\beta}{}'I_{zk}S_{z\alpha}S_{z\beta},$$

and

$$[G_{\pm1}{}^1,G_{\mp2}]=\sum_\beta\sum_{k>j}\{jk\beta\}_\mp{}'+\{kj\beta\}_\mp{}',$$

where

$$\{jk\beta\}_\mp{}'=\pm2D_{jk}{}'C_{k\beta}{}'I_{\mp j}I_{zk}S_{z\beta}.$$

Multiplying the appropriate commutators and summing over all subscripts we obtain for the traces eval-

uated in the spherical basis[21]

$$A'=[S(S+1)/6N_I]\sum_{k,\beta}C_{k\beta}{}^2,$$

$$B'=(1/9N_I)\sum_\beta\sum_{k>j}[-(11/4)A_{jk}{}^2C_{j\beta}{}^2+5A_{jk}{}^2C_{j\beta}C_{k\beta}]$$

$$\times S(S+1)I(I+1)$$

$$-(1/36N_I)\sum_k\sum_{\beta>\alpha}a_{\alpha\beta}{}^2(C_{k\alpha}-C_{k\beta})^2S^2(S+1)^2,$$

$$C'=(1/60N_I)\sum_{k,\beta}C_{k\beta}{}^4(3S^2+3S-1)S(S+1)$$

$$+(1/18N_I)\sum_k\sum_{\alpha>\beta}C_{k\alpha}{}^2C_{k\beta}{}^2S^2(S+1)^2,$$

$$D=(1/16N_I)\sum_\beta\sum_{k>j}C_{k\beta}{}^2A_{jk}{}^2I(I+1)S(S+1),$$

$$E=-(1/8N_I)\sum_\beta\sum_{k>j}A_{jk}{}^2(C_{k\beta}{}^2+C_{j\beta}{}^2)I(I+1)S(S+1),$$

$$F=G$$

$$=(1/9N_I)\sum_\beta\sum_{k>j}\{\tfrac{3}{8}A_{jk}{}^2(C_{j\beta}{}^2+C_{k\beta}{}^2)+\tfrac{3}{2}A_{jk}{}^2C_{j\beta}C_{k\beta}\}$$

$$\times I(I+1)S(S+1).$$

The lattice sums required to obtain numerical evaluation have been calculated on an electronic computer for the static magnetic field along the three principal axes in a single crystal of NaF. The lattice constant used in these sums is $a=4.620$ Å. The sums involving $P_{jk}{}^2$ include all interactions out to 248 nearest-neighbor Na nuclei. This corresponds to the 12 nearest-neighbor Na shells or 21 shells including both F and Na nuclei. The sums involving $P_{j\alpha}{}^2$ include all interactions out

[21] E. Ambler, J. C. Eisenstein, and J. F. Schooley, J. Math. Phys. 3, 760 (1962).

to the ninth fluorine shell (nineteenth shell counting both F and Na nuclei). This corresponds to 236 F nuclei. For both types of single sum the contribution from the remainder of the spins in the lattice is estimated by an isotropic integration. This is less than 1.0% in each case. The integrated contribution to the single sum of type $P_{j\alpha}{}^4$ is less than 0.005%. Integrated contributions to the double or triangular sums have not

been calculated. From the convergence of the lattice sums, we estimate that the asymptotic value differs from our truncated value by less than 10%.

The lattice sums required to evaluate all the quantities appearing in this paper are presented in Table I. Using these results, the numerical values of the quantities appearing in Secs. II A and II B have been calculated and are given in Table II.

Comparison of Average-Potential Models and Binary-Collision Models of Axial Channeling and Blocking

J. U. ANDERSEN AND L. C. FELDMAN

Bell Telephone Laboratories, Murray Hill, New Jersey 07974

(Received 26 June 1969)

A comparison is made of three types of calculations of the axial "channeling dip": the large decrease in yield of close-encounter processes for energetic ions incident on a single crystal parallel to a low-index direction. The models, indicated as (1) the binary-collision model, (2) the halfway-plane model, and (3) the continuum model, are used to calculate the dip for two standard cases corresponding to recent experiments. The methods are compared as to treatment of potential and treatment of thermal vibrations. The ease of calculation versus quantitative accuracy for the different methods is discussed, and finally the agreement with experimental results is briefly reviewed.

INTRODUCTION

ONE of the most striking and useful channeling effects observed is the almost complete extinction of close-encounter processes for energetic ions incident on a single crystal parallel to a low-index direction. A large amount of experimental information is becoming available on this "string effect," for a variety of combinations of Z_1, Z_2, E, and T, where Z_1 and Z_2 are the atomic numbers of the incident particles and the crystal atoms, respectively, E is the particle energy, and T is the crystal temperature.

Several authors[1-5] have contributed to the understanding of this phenomenon in terms of the motion of channeled particles in an average string, or row, potential. The most detailed and comprehensive treatment has been given by Lindhard,[3] and Linhard *et al.*[6] The important question of applicability of classical mechanics was discussed, and it was concluded that for channeling of heavy particles (protons, α-particle, etc.) classical orbital pictures may be used. From a discussion of the validity of the continuum model, simple estimates

of the critical angle resulted. An important modification to the continuum model is the halfway-plane description introduced in Appendix A of Ref. 3. On the basis of this description and a simple model for the influence of thermal vibrations, formulas for the angular distribution of particles emitted from a string atom were obtained. These "blocking" formulas also apply to channeling experiments, where the yield of a close-encounter process is measured as a function of incidence angle of the beam with respect to a string direction. This is a consequence of the rule of reversibility as discussed in Ref. 3. Recently, a systematic numerical evaluation of these formulas has been made.[7,8]

Some of the early blocking results[9,10] were interpreted in terms of a simple two-body model, where the emitted particle only interacts with the nearest neighbor on the string. The use of high-speed computers has made it possible to extend this two-body model and take into account binary collisions with all string atoms. Thermal vibrations may be taken into account by letting all string atoms vibrate independently. Such calculations

[1] R. S. Nelson and M. W. Thomson, Phil. Mag. **8**, 1677 (1963).

[2] C. Lehmann and G. Leibfried, J. Appl. Phys. **34**, 2821 (1963).

[3] J. Lindhard, Kgl. Danske Videnskab. Selskab, Mat.-Fys. Medd. **34** (1965).

[4] C. Erginsoy, Phys. Rev. Letters **15**, 360 (1965).

[5] A. F. Tulinov, Dokl. Akad. Nauk SSSR **162**, 546 (1965) [English transl.: Soviet Phys.—Doklady **10**, 463 (1965)].

[6] P. Lervig, J. Lindhard, and V. Nielsen, Nucl. Phys. **A96**, 481 (1967).

[7] J. U. Andersen, Kgl. Danske Videnskab. Selskab, Mat.-Fys. Medd. **36** (1967).

[8] Because of the finite step size in the integration, an error of $\sim 5\%$ was inherent in these calculations. In more accurate calculations, the width is increased by $\sim 0.05\psi_1$. This explains the small discrepancy between results in this paper and those in Ref. 7.

[9] D. S. Gemmel and R. E. Holland, Phys. Rev. Letters **14**, 945 (1965).

[10] O. S. Oen, Phys. Letters **19**, 358 (1965).